R. J. Comparin
Assistant Professor.
Dept. of Mech. Eng.,
University of Wisconsin,
1513 University Ave.,
Madison, WI 53706

R. Singh
Professor.
Dept. of Mech. Eng.,
The Ohio State University,
206 W 18th Ave.,
Columbus, OH 43210

An Analytical Study of Automotive Neutral Gear Rattle

A reduced order nonlinear model of an automotive manual transmission is presented and the neutral rattle case is analyzed. For a single frequency excitation and primary resonance, approximate analytical solutions are developed for a multi-degree-of-freedom model of a transmission using the method of harmonic balance. Based on these solutions, a simplified set of equations is developed for the study of neutral gear rattle and the use of these equations for design studies is illustrated. The nonlinear frequency response characteristics are discussed and the results are compared to similar studies described in the literature. It is shown that this analysis provides an improved understanding of the neutral gear rattle problem as well as an analytical basis for the nonlinear behavior reported in the literature.

Introduction

Gear rattle is a major source of noise and vibration in automotive manual transmissions and is characterized by backlash induced vibro-impacts between meshing gears. Torsional vibration, caused by engine torque pulses, results in cyclic angular accelerations of the components in the geared system. At a gear mesh, when the inertia torque of the driven member exceeds the load torque, gear tooth separations and impacts occur. Repeated impacts, referred to as vibro-impact or rattle, may lead to excessive noise and large dynamic tooth loads. To relate vibro-impact to gear noise and gear vibration level (gear rattle level) or dynamic stress, one must not only be able to predict the onset of vibro-impact but also the dynamic behavior of the system during vibro-impact.

A number of investigators have studied gear rattle; Nakamura (1967), Wang (1977), Hayashi et al. (1979), and Yang and Lin (1987) studied vibro-impact between two gears; Setter (1969), Azar and Crossley (1975, 1977), Hedges et al. (1979), Wang (1980), and Okada et al. (1981) considered systems with flexible shafts as well as gear pairs; and finally Sakai et al. (1981), Seaman et al. (1984), Ohuma et al. (1985), Fujimoto et al. (1987), Reik (1986), Drexl (1987), Fudala et al. (1987), and Xie et al. (1989) considered gear rattle in automotive manual transmissions. Gear rattle has been found to be a nonlinear steady state vibration problem which generally occurs at or near system resonant frequencies. It was also found that gear rattle levels (vibration levels) could be given in terms of the mean square value of the displacement or acceleration and that impact transients could be ignored. Experimental studies of actual transmissions, as reported by Sakai et al. (1981) Seaman et al. (1984), Ohnuma et al. (1985), and Fujimoto et al. (1987), have shown that gear rattle is affected by the amount of backlash, the stiffness and damping in the clutch, the drag load on the gears (viscous drag from journal bearings), and the distribution of inertia in the transmission.

Although some of the general characteristics of gear rattle in automotive transmissions are known, no specific analytical models are available which can be used to understand the dynamic behavior of the transmission system. In addition, because previous studies have generally been based on simple linear models and/or the results from nonlinear digital and analog simulations, the global design concepts are understood but the effects of system nonlinearities on these concepts are not. To conduct a more comprehensive study for obtaining a better understanding of the nonlinear dynamic characteristics of the transmission system, a close form analytical solution would generally be required. Exact solutions are not available, therefore, approximate analytical solutions must be developed which, when applied systematically and correctly, can be used to study the dynamic behavior.

The objectives of this analysis are summarized as follows: (*1*) Develop approximate analytical solutions for the nonlinear frequency response of a multi-degree-of-freedom model of an automobile manual transmission, (*2*) Simplify these solutions to obtain formulations which are suitable for the study of neutral gear rattle, and (*3*) Illustrate the use of the simplified formulations for developing design guidelines for reduced rattle.

Formulation of the Governing Equations

A reduced order model of the automotive transmission is shown in Fig. 1. It was shown by Comparin (1988) that the four degree of freedom lumped parameter model is sufficient for the study of neutral gear rattle; similar models have been used by other investigators [Sakai et al. (1981), Ohnuma et al. (1985), Fujimoto et al. (1987), and Xie et al. (1989)]. The model consists of a flywheel-clutch (I–II) system coupled to a gear pair (III–IV) with a flexible shaft where the shaft stiffness, K_2, is chosen to correspond to the lowest shaft torsional mode in the actual transmission system. The moment of inertia I_m includes the reflected inertia of the other elements of the transmission. In the most general model, there are three nonlinear stiffness elements: the multi-stage stiffness of the clutch, $K_1 f_1$ (δ_1), and the backlash in the clutch spline and

Contributed by the Power Transmission and Gearing Committee for publication in the JOURNAL OF MECHANICAL DESIGN. Manuscript received July 1989.

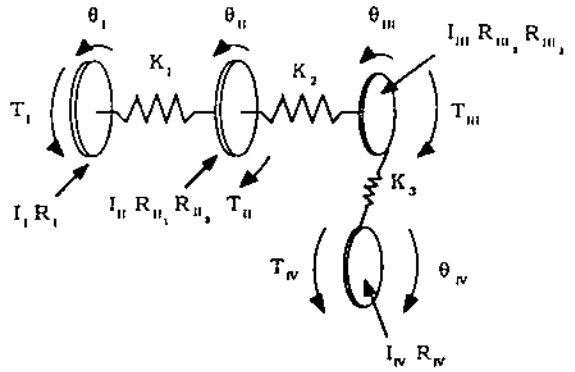

Fig. 1 Generalized four degree-of-freedom system. I—flywheel, II—clutch, III—input gear, and IV—output gear

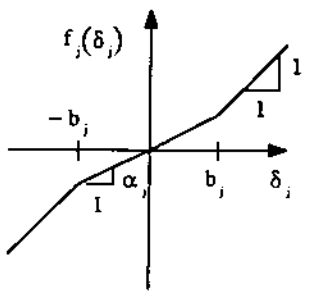

Fig. 2 Force displacement relationship for nonlinear stiffness $f_j(\delta_j)$

gear pair, $K_2 f_2(\delta_2)$ and $K_3 f_3$ (δ_3), respectively. A generic nonlinear element $f_j(\delta_j)$, referred to as a clearance type nonlinearity, is shown in Fig. 2. Here α_j is a measure of the strength of the nonlinearity. When α_j is close to one the system is weakly nonlinear and when α_j is much greater or much less than one the system is strongly nonlinear. For the clutch nonlinearity, α_1 is nonzero and in general $\alpha_1 << 1$ and for backlash $\alpha_3 = 0$. Therefore, a multi-stage clutch and backlash represent examples of strong nonlinearities.

In the absence of damping, the equations of motion for the transmission system are given by:

$$I_I\ddot{\theta}_I + K_1 f_1(\delta_1) R_I = T_I \tag{1a}$$

$$I_{II}\ddot{\theta}_{II} - K_1 f_1(\delta_1) R_{II_1} + K_2 f_2(\delta_2) R_{II_2} = -T_{II} \tag{1b}$$

$$I_{III}\ddot{\theta}_{III} - K_2 f_2(\delta_2) R_{III_2} + K_3 f_3(\delta_3) R_{III_3} = -T_{III} \tag{1c}$$

$$I_{IV}\ddot{\theta}_{IV} - K_3 f_3(\delta_3) R_{IV} = -T_{IV} \tag{1d}$$

where:

$$\delta_1 = \theta_I R_I - \theta_{II} R_{II_1};\ \delta_2 = \theta_{II} R_{II_2} - \theta_{III} R_{III_2};$$

$$\delta_3 = \theta_{III} R_{III_3} - \theta_{IV} R_{IV}$$

$$f_j(\delta_j) = \begin{cases} \delta_j - (1-\alpha_j) b_j, & b_j < \delta_j \\ \alpha_j \delta_j, & -b_j \le \delta_j \le b_j \\ \delta_j + (1-\alpha_j) b_j, & \delta_j < -b_j \end{cases}$$

In the equations of motion, R_{i_j} refers to the characteristic radius of the ith inertia associated with jth stiffness element. For the transmission system, $R_I = R_{II_1}$ and represents the radius where the coil springs in the clutch are located; $R_{II_2} = R_{III_2}$ and represents the pitch radius of the clutch spline; and R_{III_3} and R_{IV} represent the pitch radii of the input and output gears, respectively. The input torque T_I is composed of a mean component, T_{mI}, associated with the torque transmitted through the transmission and an altermating component, T_{pI}, associated with the engine torque pulses. The other torques, T_{II}, T_{III}, and T_{IV} have a mean component only and represent drag torques on the different components due to friction in the system.

The multi-degree-of-freedom (MDOF) system is semi-definite and the equations of motion can be simplified by rewriting equation (1) in terms of the relative displacement, δ_j, between the inertia elements. In addition, backlash is usually defined as a length and not an angle so the equations of the motion are rewritten in terms of an analogous translation system.

$$M_1\ddot{\delta}_1 + K_1 f_1(\delta_1) - K_2 \frac{M_1}{M_{II_1}} \frac{R_{II_2}}{R_{II_1}} f_2(\delta_2) = F_{m1} + F_p(t) \tag{2a}$$

$$M_2\ddot{\delta}_2 + K_2 f_2(\delta_2) - K_1 \frac{M_2}{M_{II_2}} \frac{R_{II_1}}{R_{II_2}} f_1(\delta_1) - K_3 \frac{M_2}{M_{III_2}} \frac{R_{III_3}}{R_{III_2}} f_3(\delta_3) = F_{m2} \tag{2b}$$

$$M_3\ddot{\delta}_3 + K_3 f_3(\delta_3) - K_2 \frac{M_3}{M_{III_3}} \frac{R_{III_2}}{R_{III_3}} f_2(\delta_2) = F_{m3} \tag{2c}$$

where:

Nomenclature

b = break points for stages in a general clearance nonlinearity
$f(\ )$ = general nonlinear function
F = force
I = inertia
K = general stiffness term
M = mass
N_{fm} = describing function for mean component
N_{fp} = describing function for alternating component
R = radius
T = torque
t = time
α = stiffness ratio
$\delta, \dot{\delta}, \ddot{\delta}$ = relative displacement, velocity, and acceleration
η = hysteretic damping factor
$\theta, \dot{\theta}, \ddot{\theta}$ = angular displacement, velocity, and acceleration
ϕ = phase angle
μ = generalized argument of describing function
φ = generalized phase angle $(\varphi = \Omega t + \phi)$
ω = angular frequency (rad/sec)
ω_n = natural frequency (rad/sec)
Ω = angular frequency of external excitation (rad/sec)
Ω_N = resonance frequency
Ω_{ij} = stiffness coefficient for multi-degree-of-freedom case

Subscripts

F_p = excitation force
m = mean
p = alternating component

Superscripts

$(\dot{\ })$ = first derivative with respect to time
$(\ddot{\ })$ = second derivative with respect to time
$(\bar{\ })$ = nondimensional variable

$$M_{i_j} = \frac{I_i}{R_{i_j}^2};\ i = \text{I, II, III, IV}\ j = 1, 2, 3$$

$$M_1 = \frac{M_{\text{I}} M_{\text{II}_1}}{M_{\text{I}} + M_{\text{II}_1}};\ M_2 = \frac{M_{\text{II}_2} M_{\text{III}_2}}{M_{\text{II}_2} + M_{\text{III}_2}};\ M_3 = \frac{M_{\text{III}_3} M_{\text{IV}}}{M_{\text{III}_3} + M_{\text{IV}}}$$

$$F_{m1} = \frac{T_{m\text{I}} M_1}{R_{\text{I}} M_{\text{I}}} + \frac{T_{m\text{II}} M_1}{R_{\text{II}_1} M_{\text{II}_1}};\ F_{m2} = -\frac{T_{m\text{II}} M_2}{R_{\text{II}_2} M_{\text{II}_2}}$$

$$+ \frac{T_{m\text{III}} M_2}{R_{\text{III}_2} M_{\text{III}_2}}\ F_{m3} = -\frac{T_{m\text{III}} M_3}{R_{\text{III}_3} M_{\text{III}_3}} + \frac{T_{m\text{IV}} M_2}{R_{\text{IV}} M_{\text{IV}}};$$

$$F_p = \frac{T_{p\text{I}} M_1}{R_{\text{I}} M_{\text{I}}}$$

Here the nonlinear functions $f_j(\delta_j)$, $j = 1, 2, 3$ are defined in terms of a stiffness break point b_j and a relative stiffness between the stages α_j as shown in Fig. 2. The equations of motion are nondimensionalized as follows: length $\bar{\delta}_j = \delta_j / b\ \bar{b}_j = b_j / b$, time $\bar{t} = t\omega_{11}$ where $\omega_{11}^2 = K_1 / M_1$, force $\bar{F}_{mj} = F_{mj} / M_j b\omega_{11}^2$, $\bar{F}_p = F_p / M_1 b\omega_{11}^2$ and frequency $\bar{\Omega} = \Omega / \omega_{11}$, $\bar{\Omega}_{ij} = K_{ij} / M_i \omega_{11}$ where K_{ij}, $i = 1, 2, 3$, and $j = 1, 2, 3$ are the coefficients of $f_j(\delta_j)$ in the ith equation, respectively. The value b is any characteristic dimension of the system. The nondimensional equations of motion become:

$$\begin{bmatrix} 1 & 0 & 0 \\ 0 & 1 & 0 \\ 0 & 0 & 1 \end{bmatrix} \begin{Bmatrix} \ddot{\bar{\delta}}_1 \\ \ddot{\bar{\delta}}_2 \\ \ddot{\bar{\delta}}_3 \end{Bmatrix} + \begin{bmatrix} \bar{\Omega}_{11}^2 & -\bar{\Omega}_{12}^2 & 0 \\ -\bar{\Omega}_{21}^2 & -\bar{\Omega}_{22}^2 & -\bar{\Omega}_{23}^2 \\ 0 & -\bar{\Omega}_{32}^2 & \bar{\Omega}_{33}^2 \end{bmatrix} \begin{Bmatrix} f_1(\delta_1) \\ f_2(\delta_2) \\ f_3(\delta_3) \end{Bmatrix}$$

$$= \begin{Bmatrix} \bar{F}_{m1} + \bar{F}_p \\ \bar{F}_{m2} \\ \bar{F}_{m3} \end{Bmatrix} \tag{3a}$$

$$f_j(\bar{\delta}_j) = \begin{cases} \bar{\delta}_j - (1-\alpha_j)\bar{b}_j & , \quad \bar{b}_j < \bar{\delta}_j \\ \alpha_j \bar{\delta}_j & , \quad -\bar{b}_j \le \bar{\delta}_j \le \bar{b}_j \\ \bar{\delta}_j + (1-\alpha_j)\bar{b}_j & , \quad \bar{\delta}_j < -\bar{b}_j \end{cases} \tag{3b}$$

Steady State Solution

The method of harmonic balance is used to obtain an approximate analytical solution of the MDOF system given by equation (3). A complete description of the method of harmonic balance is given by Gelb and Vander Velde (1968). The method of harmonic balance was selected for two reasons: an apriori assumption regarding the strength of the nonlinearity (magnitude of α) is not required, and the method is well suited to the study of nonlinearities described by nonanalytic functions. The excitation is assumed to have the following form:

$$\bar{F}_1 = \bar{F}_{m1} + \bar{F}_p \cos(\bar{\Omega}_p \bar{t} + \phi_{F_p}),\ \bar{F}_2 = \bar{F}_{m2}, \text{ and } \bar{F}_3 = \bar{F}_{m3} \tag{4}$$

Here $\bar{F}_{mj}$ represents the mean transmitted force associated with each relative displacement and $\bar{F}_p$ is the amplitude of the vibratory component acting on the first inertia at frequency $\bar{\Omega}_p$ and relative phase angle ϕ_{F_p}. The approximate solution is assumed to have the form:

$$\bar{\delta}_j = \bar{\delta}_{mj} + \bar{\delta}_{pj} \cos(\bar{\Omega}_p \bar{t} + \phi_{pj}),\ j = 1, 2, 3 \tag{5}$$

The constant term $\bar{\delta}_{mj}$ is used to account for the steady state offset, or bias, introduced by the mean load component $\bar{F}_{mj}$. The term $\bar{\delta}_{pj}$ is the forced response due to the alternating force $\bar{F}_p$. The solution given by equation (5) assumes that the forced response of equation (3) is given by the first harmonic only and, therefore, neglects not only the higher harmonics and the possibility of superharmonics or subharmonics but also the possibility of combination resonances and internal resonances.

The nonlinearities $f_j(\bar{\delta}_j)$ are expanded in a Fourier series, retaining only the mean and first harmonic terms for each nonlinearity. The nonlinear functions are given in terms of the describing functions N_{fmj} and N_{fpj} are defined as:

$$f_j(\bar{\delta}_j) = N_{fmj}\bar{\delta}_{mj} + N_{fpj}\bar{\delta}_{pj}\cos\varphi_{pj},\ j = 1, 2, 3 \tag{6a}$$

$$N_{fmj}(\bar{\delta}_{mj}, \bar{\delta}_{pj}) = \frac{1}{\pi\bar{\delta}_{mj}} \int_0^{\pi} f_j(\bar{\delta}_j) d\varphi_{pj} \tag{6b}$$

$$N_{fpj}(\bar{\delta}_{mj}, \bar{\delta}_{pj}) = \frac{2}{\pi\bar{\delta}_{pj}} \int_0^{\pi} f_j(\bar{\delta}_j) \cos\varphi_{pj} d\varphi_{pj} \tag{6c}$$

$$\varphi_{pj} = \bar{\Omega}_p \bar{t} + \phi_{pj} \tag{6d}$$

The describing functions are simply the Fourier coefficients divided by the corresponding displacement components $\bar{\delta}_{mj}$ and $\bar{\delta}_{pj}$.

Substituting equations (4), (5), and (6) into equation (3) and equating coefficients of like harmonics yields a set of coupled nonlinear algebraic equations. Solving these equations for $\bar{\delta}_{mj}$ and $\bar{\delta}_{pj}$ and redefining the mean components relative to the center of their respective nonlinearities yields the following set of nonlinear algebraic equations:

$$\bar{\delta}_{mj} = \frac{\bar{F}_{mj}}{N_{fmj}},\ j = 1, 2, 3,\ \bar{F}_{m1} = \frac{T_{m1}}{R_1 b K_1} \tag{7a,b}$$

$$\bar{F}_{m2} = \frac{T_{m\text{I}} - T_{m\text{II}}}{R_{\text{II}_2} b K_2},\ \bar{F}_{m3} = \frac{T_{m\text{IV}}}{R_{\text{IV}} b K_3} \tag{7c,d}$$

$$\bar{\delta}_{p1} = \frac{\pm\dfrac{\bar{F}_p}{\bar{\Omega}_{11}^2}\left[\left(N_{fp2} - \dfrac{\bar{\Omega}_p^2}{\bar{\Omega}_{22}^2}\right)\left(N_{fp3} - \dfrac{\bar{\Omega}_p^2}{\bar{\Omega}_{33}^2}\right) - \dfrac{\bar{\Omega}_{23}^2\,\bar{\Omega}_{32}^2}{\bar{\Omega}_{22}^2\bar{\Omega}_{33}^2} N_{fp2}N_{fp3}\right]}{\Lambda} \tag{7e}$$

$$\bar{\delta}_{p2} = \frac{\pm\dfrac{\bar{F}_p\bar{\Omega}_{21}^2}{\bar{\Omega}_{11}^2\bar{\Omega}_{22}^2} N_{fp1}\left(N_{fp3} - \dfrac{\bar{\Omega}_p^2}{\bar{\Omega}_{33}^2}\right)}{\Lambda} \tag{7f}$$

$$\bar{\delta}_{p3} = \frac{\pm\dfrac{\bar{F}_p\bar{\Omega}_{32}^2\bar{\Omega}_{21}^2}{\bar{\Omega}_{11}^2\bar{\Omega}_{22}^2\bar{\Omega}_{33}^2} N_{fp1}N_{fp2}}{\Lambda},\quad \tan(\phi_{Fp} - \phi_{p1}) = \frac{0}{\bar{\delta}_{p1}\Lambda} \tag{7g,h}$$

$$\Lambda = \left\{\left[\left(N_{fp1} - \frac{\bar{\Omega}_p^2}{\bar{\Omega}_{11}^2}\right)\left(N_{fp2} - \frac{\bar{\Omega}_p^2}{\bar{\Omega}_{22}^2}\right) - \frac{\bar{\Omega}^2{}_{12}\,\bar{\Omega}_{21}^2}{\bar{\Omega}_{11}^2\bar{\Omega}_{22}^2} N_{fp1}N_{fp2}\right]\left(N_{fp3} - \frac{\bar{\Omega}_p^2}{\bar{\Omega}_{33}^2}\right) - \left(N_{fp1} - \frac{\bar{\Omega}_p^2}{\bar{\Omega}_{11}^2}\right)\frac{\bar{\Omega}_{23}^2\bar{\Omega}_{32}^2}{\bar{\Omega}_{22}^2\bar{\Omega}_{33}^2} N_{fp2}N_{fp3}\right\} \tag{7i}$$

Here a positive sign is used when $\bar{\delta}_{p1}$ and $\bar{F}_p$ are in phase and a negative sign when they are out of phase, where the relative phase, $(\phi_{Fp} - \phi_{p1})$, is defined by equation (7h). The describing functions N_{fmj} and N_{fpj} are given by equations (8a) and (8b):

$$N_{fmj} = 1 + \frac{\bar{\delta}_{pj}}{2\bar{\delta}_{mj}}\left\{(1-\alpha_j)\left[G\left(\frac{\bar{b}_j - \bar{\delta}_{mj}}{\bar{\delta}_{pj}}\right) - G\left(\frac{-\bar{b}_j - \bar{\delta}_{mj}}{\bar{\delta}_{pj}}\right)\right]\right\} \tag{8a}$$

$$N_{fpj} = 1 - \left(\frac{1-\alpha_j}{2}\right)\left[H\left(\frac{\bar{b}_j - \bar{\delta}_{mj}}{\bar{\delta}_{pj}}\right) - H\left(\frac{-\bar{b}_j - \bar{\delta}_{mj}}{\bar{\delta}_{pj}}\right)\right] \tag{8b}$$

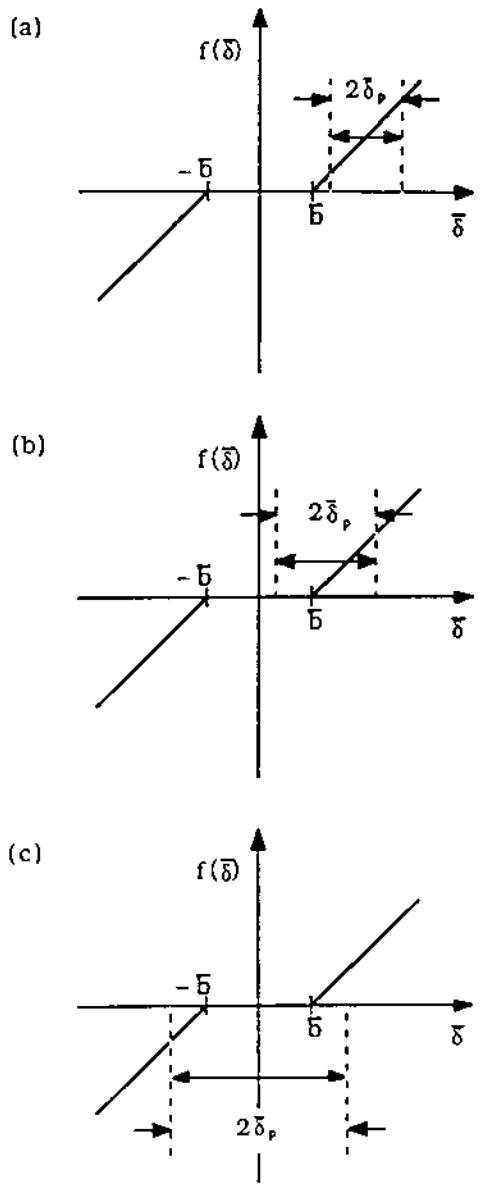

Fig. 3 Illustration of different impact regimes: *(a)* no impacts *(b)* single sided impacts *(c)* two sided impacts

$$G(\mu) = \frac{2}{\pi}(\mu \sin^{-1}\mu + \sqrt{1-\mu^2}) \quad , \ |\mu| \le 1$$
$$= |\mu| \quad , \ |\mu| > 1 \qquad (8c)$$
$$= -1 \quad , \ \mu < -1$$
$$H(\mu) = \frac{2}{\pi}(\sin^{-1}\mu + \mu\sqrt{1-\mu^2}) \quad , \ |\mu| \le 1 \qquad (8d)$$
$$= +1 \quad , \ \mu > 1 \qquad (8d)$$
$$\mu = \frac{\pm \bar{b}_j - \bar{\delta}_{mj}}{\bar{\delta}_{pj}} \qquad (8e)$$

It should be noted that in all cases, when $\alpha_j = 1$ the describing functions N_{fmj} and N_{fpj}, given by equations (8*a*) and (8*b*), reduce to one, which is the linear case.

The MDOF system can be viewed as essentially consisting of three coupled systems called impact pairs: the I-II pair, the II-III pair and the III-IV pair. To better understand the type of behavior which may be expected, consider the physical effect of the nonlinear stiffness on one of the impact pairs. The overall response can be separated into three different regimes: a no impact regime, a single sided impact regime, and a two sided impact regime. The different impact regimes are illustrated for backlash in Fig. 3.

This type of nonlinearity can be viewed as an amplitude dependent stiffness with an average value given by the relative amount of time (over one period of vibration) that the impact pair is in one stage versus the other. As the amplitude of the alternating component $\bar{\delta}_p$ changes so does the stiffness. The impact pair is said to be hardening if the stiffness increases for increasing $\bar{\delta}_p$ and softening if the stiffness decreases for increasing $\bar{\delta}_p$. For the clearance type nonlinearity, the hardening or softening character will depend on the location of the mean component and on whether the impact pair is undergoing single or two sided impacts (the system is linear for the no impact case). For single-sided impacts if the mean component (static deflection) is in the second stage, as $\bar{\delta}_p$ increases the average stiffness decreases because the amount of time the system spends in the first stage increases and the system is softening. For the two-sided impact case and the single-sided case where the mean component is in the first stage the situation is reversed and the average stiffness will increase as $\bar{\delta}_p$ increases resulting in a hardening system. Each impact pair may undergo any or all of the different impact regimes, so the MDOF system may have a total of $3 \times 3 \times 3 = 27$ cases. Further complicating the situation is the fact that the impact pairs are dynamically coupled; therefore, the behavior of a given impact pair will, in general, depend on the type of vibration experienced by the other two.

Equations (7) and (8) can be solved using a number of different numerical techniques but since the MDOF nonlinear system can exhibit a wide range of dynamic behavior, general observations and conclusions usually cannot be made without considering special cases. Further a general nonlinear analysis can be very complicated and expensive so it is useful to known when a simplified nonlinear analysis or even a linear analysis might be acceptable. Although the specific results from an analysis of special cases may not be directly applied to a wider class of problems, the general methodology introduced should be applicable. To illustrate these points consider the frequency response for the neutral rattle case.

Simplified Solution for Neutral Gear Rattle

In neutral, the clutch is generally designed as a vibration isolator [Xie et al. (1989)] and hence for low transmissibility the operating speed (idle speed) $\hat{\Omega} > \sqrt{2}\hat{\Omega}_{N1}$ where $\hat{\Omega}_{N1}$ is the resonance associated with the stiffness of first stage. In general the idle speed $\hat{\Omega}$ is fixed so the stiffness of the first stage, $\alpha_1 K_1$, must be chosen to yield an appropriate resonant frequency. Space constraints limit the amount of wind-up allowed and place a lower limit on the spring stiffness and so the idle speed $\hat{\Omega}$ will, in general, only be slightly larger than the first stage resonance $\hat{\Omega}_{N1}$. The other resonances in the transmission are associated with the shaft and mesh stiffness and will be much higher. A typical idle speed would be 15Hz with the engine torque pulse excitation at $\hat{\Omega}_p \approx 30$Hz (for a four-cylinder engine). The first shaft resonance will usually be an order of magnitude larger, (say $\hat{\Omega}_{N2} \approx 10\hat{\Omega}_p$), and the gear mesh resonances are usually two orders of magnitude larger, (say $\hat{\Omega}_{N3} \approx 100\hat{\Omega}_p$). Assuming a linear shaft stiffness K_2 (neglecting the clutch spline), it can be shown that $\hat{\Omega}_{22} >> \hat{\Omega}_p$, $\hat{\Omega}_{33} >> \hat{\Omega}_p$ and equation (7) can be simplified to yield a single mode system as shown schematically in Fig. 4. An approximate damped response is obtained by redefining the normalized excitation frequency and adding a hysteretic damping term η where it is assumed that the hysteresis can be represented by a complex stiffness in the frequency domain [see Thomson (1981)]. The resulting equations are:

$$\bar{\delta}_{mj} = \frac{\bar{F}_{mj}}{N_{fmj}}, \ j = 1, 2, 3, \ \bar{\delta}_{p1} = \frac{\bar{F}_{p1}}{\sqrt{(N_{fp1} - \hat{\Omega}_p^2)^2 + \eta^2}} \qquad (9a,b)$$

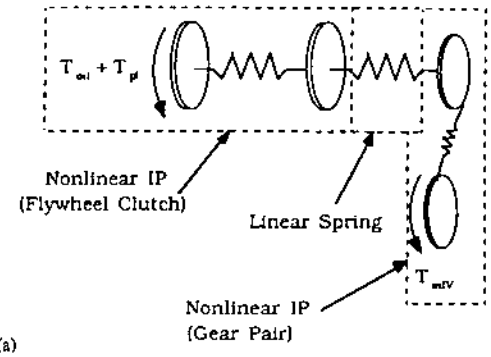

(a)

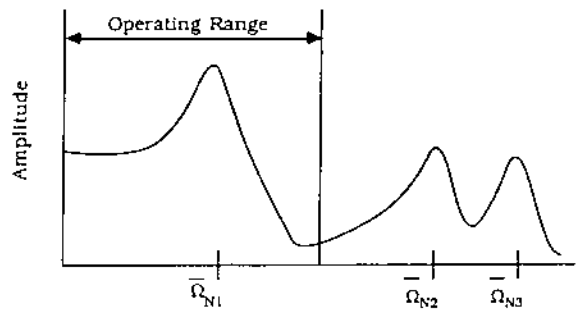

(b)

Fig. 4 Neutral rattle case (a) physical model (b) typical frequency response function

$$\delta_{p2} = \frac{\bar{F}_{p2} N_{fp1}}{\sqrt{(N_{fp1} - \bar{\Omega}_p^2)^2 + \eta^2}}, \quad \delta_{p3} = \frac{\bar{F}_{p3}\left(\frac{N_{fp1}}{N_{fp3}}\right)}{\sqrt{(N_{fp1} - \bar{\Omega}_p^2)^2 + \eta^2}} \tag{9c,d}$$

where:

$$\bar{F}_{p1} = \frac{\bar{F}_p}{\bar{\Omega}_{11}^2(1 - \bar{\Omega}_{c1}^2)} \quad \bar{F}_{p2} = \frac{\bar{F}_p \bar{\Omega}_{21}^2}{\bar{\Omega}_{11}^2 \bar{\Omega}_{22}^2}\left(\frac{\bar{\Omega}_{c2}^2}{1 - \bar{\Omega}_{c1}^2}\right) \tag{9e,f}$$

$$\bar{F}_{p3} = \frac{\bar{F}_p \bar{\Omega}_{32}^2 \bar{\Omega}_{21}^2}{\bar{\Omega}_{11}^2 \bar{\Omega}_{22}^2 \bar{\Omega}_{33}^2}\left(\frac{\bar{\Omega}_{c2}^2}{1 - \bar{\Omega}_{c1}^2}\right) \quad \bar{\Omega}_p^2 = \frac{\Omega_p^2}{1(-\bar{\Omega}_{c1}^2)\omega_{11}^2} \tag{9g,h}$$

$$\bar{\Omega}_{c1}^2 = \frac{\bar{\Omega}_{33}^2 \bar{\Omega}_{12}^2 \bar{\Omega}_{21}^2}{\bar{\Omega}_{11}^2(\bar{\Omega}^2{}_{22}\bar{\Omega}_{33}^2 - \bar{\Omega}_{23}^2 \bar{\Omega}_{32}^2)} \quad \bar{\Omega}_{c2}^2 = \frac{\bar{\Omega}_{22}^2 \bar{\Omega}_{33}^2}{\bar{\Omega}_{22}^2 \bar{\Omega}_{33}^2 - \bar{\Omega}_{23}^2 \bar{\Omega}_{32}^2} \tag{9i,j}$$

From an examination of equation (9) it is clear that for neutral rattle, the frequency response of the flywheel-clutch system δ_{p1} is given by the frequency response of a single impact pair. In addition, the response δ_{p1} is independent of δ_{p2} and δ_{p3} and, as a result, the behavior of the clutch can be studied independently from the gear pair. Once the behavior of the flywheel-clutch system is known then the behavior of the gear pair can be found. Therefore, the analysis of the netural gear rattle problem can be reduced to an analysis of a single impact pair. A complete discussion of the response of a single impact pair is given by Comparin and Singh (1989).

For the neutral case, the clutch resonant frequency $\bar{\Omega}_{N1}$ is usually made as slow as possible relative to the idle speed $\bar{\Omega}$ so that the clutch behaves as a vibration isolator [Fujimoto et al. (1987), Reik (1986), Xie et al. (1989) etc.]. The operating speed is essentially constant so the design objective is to select an appropriate set of system parameters such as the first stage stiffness (α_1, K_1), relative inertia (M_1), break point ($\bar{b}_1$), and hysteretic damping (η), etc. to minimize or eliminate the gear rattle problem.

To facilitate an analysis of the general characteristics of the solutions, equations (8*a* and *b*) can be modified by replacing the functions G and H with truncated series expansions [see Comparin and Singh (1989)]. The truncated series expressions which are within five percent of the original function of G and within 6 percent for H are found to be as follows for $|\mu| \leq 1$:

$$G(\mu) \cong \frac{2}{\pi}\left(1 + \left(\frac{\pi - 2}{2}\right)\mu^2\right) \tag{10a}$$

$$H(\mu) \cong \frac{4}{\pi}\left(\mu - \left(\frac{4 - \pi}{4}\right)\mu^3\right) \tag{10b}$$

Substituting the modified equations for the describing functions into equation (10) yields a simplified set of equations which are listed in the appendix. Since the dynamic behavior of the two impact pairs (the flywheel-clutch and gear pair) is of primary interest, only the equations for δ_{m1}, δ_{p1}, δ_{m3}, and δ_{p3} are given. Although these equations must still be solved numerically, the modified form is more computationally efficient and provides a better qualitative understanding of the form of the dynamic response.

Using a set of nondimensional values from an actual transmission system, the equations in the appendix are solved numerically to yield a set of typical frequency response functions which are shown in Figs. 5–7. Each figure represents a different impact condition in the clutch: specifically, no impacts, single sided impacts, and two sided impacts. The clutch behaves like a simple impact pair and for the impact cases the clutch represents a hardening system so a single jump occurs. The dynamic behavior of the gear pair follows that of the clutch but the amplitude ratio δ_{p3}/δ_{p1} varies due to impacting in the clutch as well as impacting in the gear pair.

It should be pointed out that the frequency response functions for the gear pair will appear somewhat distorted because the clearance space is very large with respect to the elastic deformation. This leads to ver large slopes in the transition regions which appear as jumps in the frequency response functions. These "apparent" jumps are different from the jump transition which occurs in the clutch. The jump transition in the clutch occurs at resonance because of the phase change between the applied force and the displacement [see Comparin and Singh (1989)]. The apparent jumps in the response of the gear pair are not related to phase changes as they do not necessarily occur at resonance. Instead they are simply a function of the magnitude of δ_{p1}.

For the cases shown in Figs. 5–7, impacting (rattle) occurs in the gear pair at the lower frequencies and at the higher frequencies a transition to no impacts occurs, as expected for a clutch designed as a vibration isolator. The design objective, therefore, is to select an appropriate set of system parameters such as the first stage stiffness (α_1, K_1), relative inertia (M_1), break point ($\bar{b}_1$), and hysteretic damping (η), etc. so that the desired idle speed is above the impact transition point.

Development of Formulations for Design

To facilitate the design process, the equations in the appendix can be used to develop additional design formulations. The design process is fairly straightforward when impacting does not occur in the flywheel-clutch system but becomes more complicated when impacting does occur. It is important, therefore, to understand the relationship between the design parameters and the transition from the no impact regime to an impact regime. According to Comparin and Singh (1989), two types of transitions can occur. The first type of transition occurs when the alternating component of the displacement increases as the excitation frequency, $\bar{\Omega}_p$, approaches resonance ($\bar{\Omega}_N \cong \sqrt{\alpha}$ or $\bar{\Omega}_N \cong 1$). The frequencies at which these transitions occur ($\bar{\Omega}_{1T}$ for the flywheel-clutch and $\bar{\Omega}_{3T}$ for the gear pair) are obtained from the equations in the appendix by

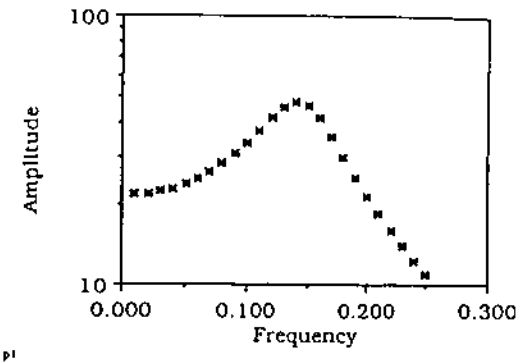

(a) $\bar{\delta}_{p1}$

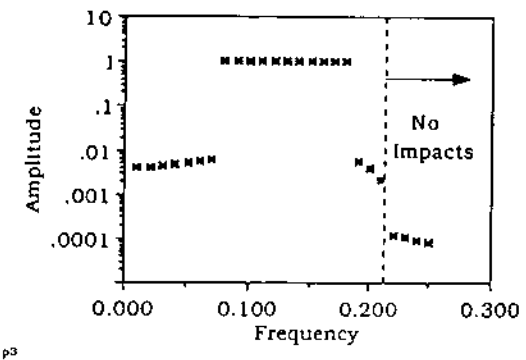

(b) $\bar{\delta}_{p3}$

Fig. 5 Frequency response functions for neutral rattle case with no impacting in the clutch. Given: $\bar{F}_{m1} = 0.1$, $\bar{F}_{m3} = 1.24 \times 10^{-4}$, $\bar{F}_{p1} = 0.48$, $\bar{F}_{p3} = 1.78 \times 10^{-4}$, $\eta = 0.01$

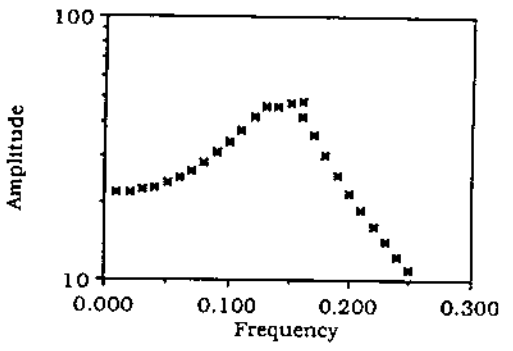

(a) $\bar{\delta}_{p1}$

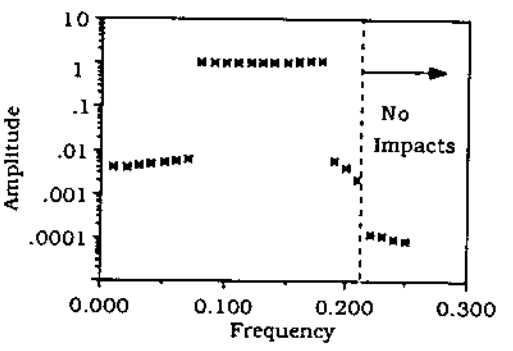

(b) $\bar{\delta}_{p3}$

Fig. 6 Frequency response functions for neutral rattle case with single sided impacting in the clutch. Given: $\bar{F}_{m1} = 0.5$, $\bar{F}_{m3} = 1.24 \times 10^{-4}$, $\bar{F}_{p1} = 0.48$, $\bar{F}_{p3} = 1.78 \times 10^{-4}$, $\eta = 0.01$

substituting in the appropriate transition displacements: $\bar{\delta}_{pj} = |\bar{b}_j - \bar{\delta}_{mj}|$ for the transiton from no impacts to single-sided impacts and $\bar{\delta}_{pj} = \bar{b}_j + |\bar{\delta}_{mj}|$ for the transition from single-sided impacts to two-sided impacts. The resulting equations for the transition from no impacts to single-sided impacts are given as:

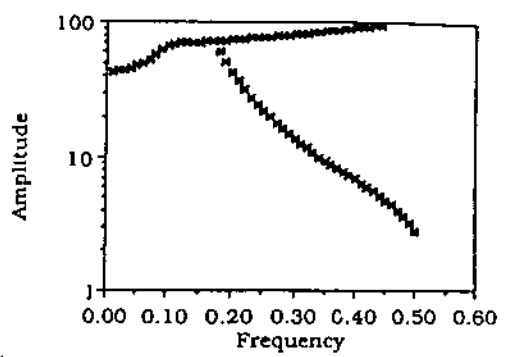

(a) $\bar{\delta}_{p1}$

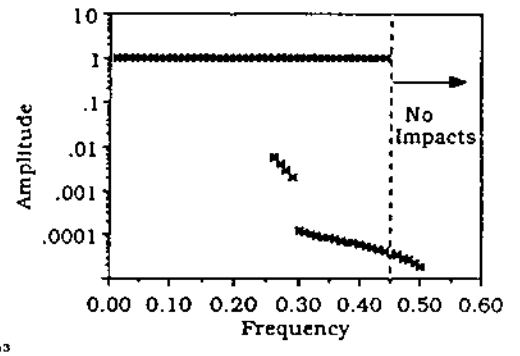

(b) $\bar{\delta}_{p3}$

Fig. 7 Frequency response functions for neutral rattle case with two sided impacting in the clutch. Given: $\bar{F}_{m1} = 0.1$, $\bar{F}_{m3} = 1.24 \times 10^{-4}$, $\bar{F}_{p1} = 0.96$, $\bar{F}_{p3} = 3.56 \times 10^{-4}$, $\eta = 0.01$

Type 1:

$$\bar{\Omega}_{1T01} = \left[\alpha_1 \pm \sqrt{\left(\frac{\bar{F}_{p1}\alpha_1}{\alpha_1 \bar{b}_1 - \bar{F}_{m1}}\right)^2 - \eta^2}\right]^{1/2} \tag{11a}$$

$$\bar{\Omega}_{3T01} = \left[N_{fp1} \pm \sqrt{\left(\frac{\bar{F}_{p3}N_{fp1}}{\alpha_3 \bar{b}_3 - \bar{F}_{m3}}\right)^2 - \eta^2}\right]^{1/2} \tag{11b}$$

Type 2:

$$\bar{\Omega}_{1T01} = \left[1 \pm \sqrt{\left(\frac{\bar{F}_{p1}}{\bar{F}_{m1} - \alpha_1 \bar{b}_1}\right)^2 - \eta^2}\right]^{1/2} \tag{11c}$$

$$\bar{\Omega}_{3T01} = \left[N_{fp1} \pm \sqrt{\left(\frac{\bar{F}_{p3}N_{fp1}}{\bar{F}_{m3} - \alpha_3 \bar{b}_3}\right)^2 - \eta^2}\right]^{1/2} \tag{11d}$$

The equations for the transition from single-sided impacts to two-sided impacts are:

$$\bar{\Omega}_{1T12} = \left[N_{fp1T} \pm \sqrt{\left(\frac{\bar{F}_{p1}}{\bar{\delta}_{p1T}}\right)^2 - \eta^2}\right]^{1/2} \tag{12a}$$

$$\bar{\Omega}_{3T12} = \left[N_{fp1} \pm \sqrt{\left(\frac{\bar{F}_{p3}N_{fp1}}{N_{fp3T}\bar{\delta}_{p3T}}\right)^2 - \eta^2}\right]^{1/2} \tag{12b}$$

$$N_{fp1T} = 1 - \frac{4}{\pi}(1-\alpha_1)\left[\frac{\bar{b}_1}{\bar{\delta}_{p1T}} - \left(\frac{4-\pi}{4}\right)\left(\frac{\bar{b}_1^3 + 3\bar{b}_1(\bar{\delta}_{p1T} - b_1)^2}{\bar{\delta}_{p1T}^3}\right)\right] \tag{12c}$$

$$\bar{\delta}_{p1T} = \frac{\{[(\bar{b}_1 + \bar{F}_{tsm1}) + \bar{F}_{m1}] + \sqrt{[(\bar{b}_1 + \bar{F}_{tsm1}) + \bar{F}_{m1}]^2 - 4\bar{F}_{tsm1}\bar{b}_1}\}}{2} \tag{12d}$$

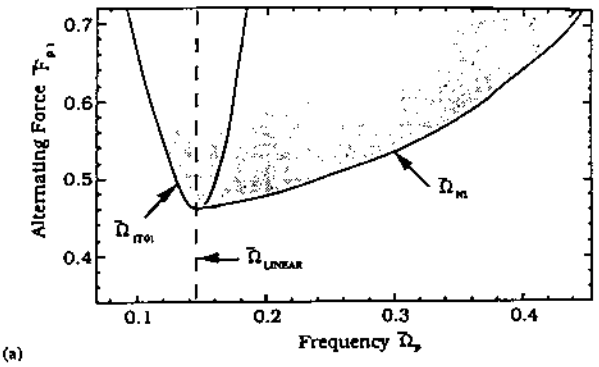

(a)

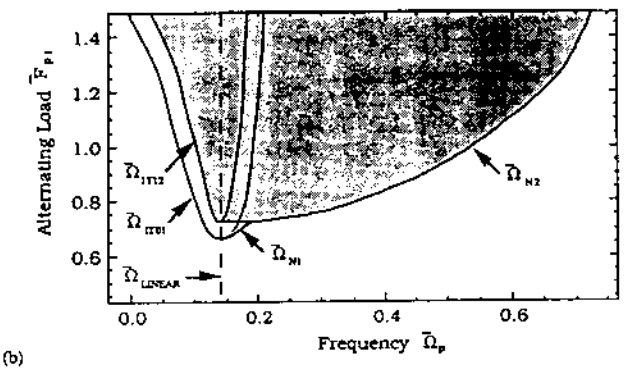

(b)

Fig. 8 Impact transitions for the clutch as a function of $\bar{F}_{p1}$ for two different values of $\bar{F}_{m1}$: (a) $\bar{F}_{m1} = 0.5$ (b) $\bar{F}_{m1} = 0.1$. The unshaded region corresponds to no impacts, the lightly shaded regions to single sided impacts, and the darkly shaded regions to two sided impacts. The linear resonance frequency corresponds to the first stage stiffness of the clutch.

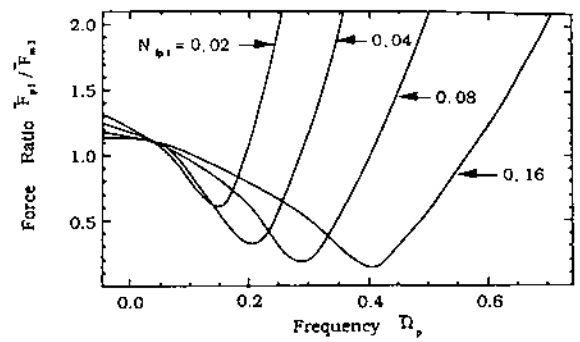

Fig. 9 Impact transition between no impacts and single sided impacts for the gear pair as a function of $\bar{F}_{p3}/\bar{F}_{m3}$ for different values of N_{fp1}. Regions below the curves corresponds to no impacts regimes and regions above the curves to impact regimes.

$$N_{fp3T} = 1 - \frac{4}{\pi}(1-\alpha_3)\left[\frac{\bar{b}_3}{\bar{\delta}_{p3T}} - \left(\frac{4-\pi}{4}\right)\left(\frac{\bar{b}_3^3 + 3\bar{b}_3(\bar{\delta}_{p3T} - \bar{b}_3)^2}{\bar{\delta}_{p3T}^3}\right)\right] \tag{12e}$$

$$\bar{\delta}_{p3T} = \frac{\{[(\bar{b}_3 + \bar{F}_{tsm3}) + \bar{F}_{m3}] + \sqrt{[(\bar{b}_3 + \bar{F}_{tsm3} + \bar{F}_{m3}]^2 - 4\bar{F}_{tsm3}\bar{b}_3}\}}{2} \tag{12f}$$

$$\bar{F}_{tsmj} = \frac{2(\pi-2)}{\pi}(1-\alpha_j)\bar{b}_j \tag{12g}$$

In equations (11), (12*a*), and (12*b*) the negative sign refers to the transition below the linear resonant frequency and the positive sign the transition above the linear resonant frequency. For the linear case, $\alpha_j = 1$, therefore is no meaning to these frequencies.

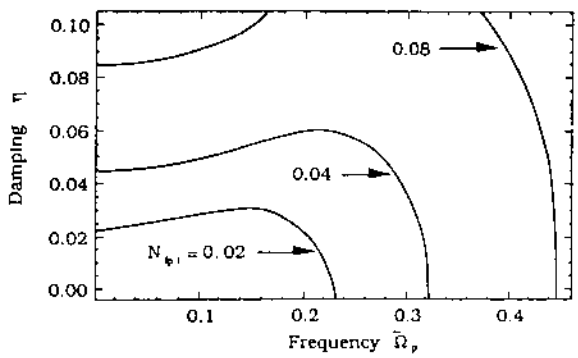

Fig. 10 Impact transition between no impacts and single sided impacts for the gear pair as a function of η for different values of N_{fp1} with $\bar{F}_{p3}/\bar{F}_{m3}$ constant. Regions above the curves correspond to no impacts regimes and regions below the curves to impact regimes.

The second type of transition is the jump transition which occurs at resonance because of the phase change between the applied force and the displacement. The jump transitions are associated with the nonlinear stiffness in the clutch. The resonant frequency is defined as the minimum of the denominator of equation (9*b*) and there are two such frequencies: one for the single sided impact case and one for the two sided impact case. The resonant frequencies are given below where $\hat{\Omega}_{N1}$ is for single sided impacts and $\hat{\Omega}_{N2}$ is for two sided impacts.

$$\hat{\Omega}_{N1} = \sqrt{\alpha_{A1} - \frac{\bar{F}_{ss1}}{\bar{\delta}_N}}; \quad \hat{\Omega}_{N2} = \sqrt{1 - \frac{\bar{F}_{ts1}}{\bar{\delta}_N}}; \quad \bar{\delta}_N = \frac{\bar{F}_{p1}}{\eta} \tag{13a,b,c}$$

$$\bar{F}_{ssj} = \frac{2}{\pi}(1-\bar{\delta}_{mj})(1-\alpha_j)\left[1 - \left(\frac{4-\pi}{\pi}\right)\left(\frac{\bar{b}_j - \bar{\delta}_{mj}}{\bar{\delta}_{pj}}\right)^2\right] \tag{13d}$$

$$\bar{F}_{tsj} = \frac{4}{\pi}(1-\alpha_j)\bar{b}_j\left[1 - \left(\frac{4-\pi}{4}\right)\left(\frac{\bar{b}_j^2 + 3\bar{\delta}_{mj}^2}{\bar{\delta}_{pj}^2}\right)\right] \tag{13e}$$

Useful design information can be obtained by using the transition and resonant frequency equations to generate impact transmission maps. A map is generated by varying one parameter in the above equations while holding the other parameters constant. Some example maps are shown in Figs. 8-10.

The two maps in Fig. 8 illustrate the effect of different values of $\bar{F}_{p1}$ on the impact regimes for a clutch for two different cases: only single-sided impacts occur (8*a*) and both single- and two sided-impacts occur (8*b*). The shaded areas in both diagrams represent regions where impacts occur with the lightly shaded areas corresponding to single-sided impacts and the darkly shaded areas to two-sided impacts. The linear natural frequency corresponding to the first stage stiffness of the clutch is also shown.

The maps shown in Fig. 8 are consistent with the frequency response functions shown in Figs. 6 and 7. The constant excitation, $\bar{F}_{p1}$, corresponds to a horizonal line on the maps. For a small enough value of the excitation, impacts do not occur and the clutch behaves as a linear SDOF system. For larger values of the excitation, no impacts occur at the lower frequencies but at higher frequencies the constant parameter line crosses into the shaded regions and impacting occurs. These impacts will exist until the nonlinear resonant frequency is reached, as was discussed earlier, and a transition back to no impacts occurs.

The primary observation to be made is the effect of impacting on the resonant frequency. As mentioned earlier, the clearance nonlinearity in the clutch represents a hardening system; N_{fp1} represents an amplitude dependent stiffness

whose average value is given by the relative amount of time (over one period of vibration) that the clutch is operating in one stage versus the other. As a result, when impacts occur the system resonant frequency increases and this increase is proportional to an increase in $\bar{F}_{p1}$. The clutch behaves as a vibration isolator above its critical frequency, which is $\bar{\Omega}_{\text{critical}} = \sqrt{2}\bar{\Omega}_N$ for a linear system, so the net result of impacting is to increase this critical frequency.

Another observation relates to the effect of the mean load on the threshold level of the excitation required for impacts to occur. For $\bar{F}_{m1} = 0.5$ [Fig. 8(*a*)] the threshold level for impacting to occur is $\bar{F}_{p1} = 0.46$ while for $\bar{F}_{m1} = 0.1$ [Fig. 8(*a*)] the threshold level for impacting to occur is $\bar{F}_{p1} = 0.65$. Physically, an increase in the mean load moves the operating point in the clutch closer to the stiffness transition point and, therefore, a smaller value of $\bar{\delta}_{p1}$ is required for impacting to occur.

The final two maps, Figs. 9 and 10, illustrate the effects of the load ratio $\bar{F}_{p3}/\bar{F}_{m3}$ and damping η, respectively, on the transition frequency between no impacts and impacts in the gear pair. The response of the gear pair depends on the behavior of the clutch and so a number of different values of N_{fp1} are considered. A value of $N_{fp1} = 0.02$ corresponds to the linear case and $N_{fp1} \geq 0.02$ to the impact cases. The value of N_{fp1} increases with the level of the impacts. The transition curves shown here are similar in shape to the curves presented for the clutch in Fig. 8. In Fig. 9 the area above a given curve corresponds to an impact region and the area below a curve to a no impact region while the reverse is true for Fig. 10.

From Fig. 9, it is clear that to reduce or eliminate rattle, the load ratio $\bar{F}_{p3} / \bar{F}_{m3}$ should be as small as possible. Preferably this is accomplished by decreasing $\bar{F}_{p3}$ as an increase in $\bar{F}_{m3}$ increases $\bar{F}_{m1}$ and this is inconsistent with a small value of $\bar{F}_{m1}$ required for the clutch. In addition $\bar{F}_{m3}$ represents a parasitic load on the system and an arbitrarily large value may degrade the overall system performance. The value of N_{fp1} is also particularly important with regard to the gear pair and can be viewed as a nonlinear coupling term. Accordingly, N_{fp1} should be as small as possible. When impacts do not occur $N_{fp1} = \alpha_1$, the first stage stiffness of the clutch. For this case the clutch behavior is linear and the requirement for a low first stage stiffness is consistent with the design of a vibration isolator and, as expected, the impact region in Fig. 9 is small. When impacts do occur, however, $N_{fp1} = \bar{\Omega}_N^2$ and the impact region grows significantly, as discussed earlier.

Finally, from Fig. 10, two specific observations can be made regarding the effect of damping on the transition frequency. First, for a given value of N_{fp1}, a low frequency region exists where an increase in damping η will eliminate impacting but above a certain frequency (a little larger than $\sqrt{2}\bar{\Omega}_N$ for the case considered here) impacts do not occur irrespective of the amount of damping. Second, the amount of damping required to eliminate rattle below the transition frequency and the transition frequency itself both increase significantly with an increase in N_{fp1}. Both observations are consistent with a system designed as a vibration isolator.

The design maps discussed above are simply representative examples which are used to illustrate the usefulness of the approximate analytical solutions for design. A large number of additional maps can also be generated and, in fact, design maps can even be combined to create design surfaces.

Discussion of Results

From a qualitative point of view, the neutral rattle case is, in general, strongly nonlinear because the overall response of the system is dominated by the nonlinear response of the clutch. Accordingly, a study of neutral rattle requires the use of a nonlinear analysis with an emphasis on the design of the clutch. This is consistent with similar studies reported in the literature by Xie et al. (1989), Fujimoto et al. (1987), Reik (1986), Ohnuma et al. (1985), and Sakai et al. (1981), all of whom used nonlinear models as part of their studies of neutral rattle.

Because of the complexity of the nonlinear system, however, the design methodology is still based primarily on linear models. Specifically, if it is assumed that impacting does not occur, either in the clutch or at the gear pair, the nonlinear problem reduces to a linear one. Using a linear model it is possible to develop a set of equations for predicting the threshold at which rattle will begin [see Xie et al. (1989)] and Sakai et al. (1981)]. These threshold equations then form the basis of the development of design guidelines.

When impacting in the clutch is unavoidable, however, the linear models are no longer valid and it is then necessary to return to the use of nonlinear models. Because of the lack of approximate analytical solutions, the design guidelines for the nonlinear case are based on nonlinear digital and/or analog simulations [Xie et al. (1989), Fujimoto et al. (1987), Reik (1986), Ohnuma et al. (1985), and Sakai et al. (1981)], and/or experimental results from actual transmission systems [Ohnuma et al. (1985), Reik (1986), and Fujimoto et al. (1987)]. As a result, the global design concepts are understood but the effects of the system nonlinearities on these concepts are not.

The major problem for the nonlinear case involves the region of multiple steady state solutions. The region exists just above the linear natural frequency associated with the first stage of the clutch and may be in the operating region for the neutral case. If the operating point falls in this region it is possible to get a low amplitude no rattle solution, or a large amplitude rattle solution depending on the initial conditions. Different initial conditions can be generated by gradual or abrupt clutching operations and by engaging or disengaging automotive accessories such as air conditioning. Fujimoto et al. (1987), Reik (1986), and Ohnuma et al. (1985) observed a jump phenomenon associated with impacting in the clutches as well as the existence of multiple steady state solutions. While they do not provide analytical formulations for describing the region, their studies do acknowledge the importance of understanding this region for reducing rattle. Current design practice is to ensure the operating point is above and away from this region.

The analytical formulations and solution methodologies presented in this study provide an additional tool for the analysis of both the linear and nonlinear cases. For no impacting, equation (10) reduces a set of linear equations and can be used for the same threshold type analysis described by Xie et al. (1989) and Sakai et al. (1981). The analytical formulations and solution methodologies are also valid for the nonlinear case and can be used to predict the range of multiple steady state solutions and the effect of the system parameters on this region. The nonlinear behavior discussed in the previous section is consistent, not only with the nonlinear digital and analog simulations described in the literature by Xie et al. (1989), Fujimoto et al. (1987), Reik (1986), Ohnuma et al. (1985), and Sakai et al. (1981), but also with the behavior of actual automotive transmission systems as reported by Ohnuma et al. (1985), Reik (1986), and Fujimoto et al. (1987).

In summary, with respect to similar studies in the literature, our mathematical model is valid and can be used to provide not only additional design information, but is also an analytical basis for the observed nonlinear behavior of the transmission system.

Acknowledgments

The authors wish to acknowledge the Chrysler Corporation for sponsoring this study. The authors also thank D. R. Houser of The Ohio State University and T. Brown, S. Rez-

zacki, and J. Frye of the Chrysler Corporation for their assistance.

References

Azar, R. C., and Crossley, F. R. E., 1975, "An Experimental Investigation of Impact Phenomenon in Spur Gear Systems," *Proceedings of the 4th World Congress on Theory of Machines and Mechanisms*, 1, pp. 157-161.

Azar, R. C., and Crossley, F. R. E., 1977, "Digital Simulation of Impact Phenomena in Spur Gear System," ASME *Journal of Engineering for Industry*, Vol. 99, pp. 792-798.

Comparin, R. J., 1988, "A Study of the Frequency Response of Impact Pairs with Application to Automotive Gear Rattle," Ph.D. Dissertation, The Ohio State University, June 1988.

Comparin, R. J., and Singh, R., 1989, "Nonlinear Frequency Response Characteristics of an Impact Pair," *Journal of Sound and Vibration*, Vol. 133, 1.

Drexl, H. J., 1987, "Torsional Dampers and Alternative Systems to Reduce Driveline Vibrations, SAE Paper 870393.

Fudala, G. J., Engle, T. C., and Karvelis, A. V., 1987, "A Systems Approach to Reducing Gear Rattle," SAE Paper 870396.

Fujimoto, T., Chikatani, Y., Kojima, J., 1987, "Reduction of Idling Rattle in Manual Transmissions," SAE Paper, 870395.

Hayashi, T., Nishi, N., Ohno, T., and Crossley, F. R. E., 1979, "Multiple Impacts of a Cylinder Between Two Planes and of the Meshing Teeth of a Pair of Gears," *Proceedings of the 5th World Congress on the Theory of Machines and Mechanisms*, pp. 350-353.

Hedges, J. I., and Butler, K. J., 1979, "A CAD System for the Analysis of Vehicle Driveline Noise," I Mech E, Paper C121/79.

Gelb, A., ad Vander Velde, W., 1968, *Multiple-Input Describing Functions and Nonlinear System Design*, McGraw-Hill, New York, NY.

Nakamura, K., 1967, "Tooth Separations and Abnormal Noise on Power Transmission Gears," Bulletin of JSME, 10.

Ohnuma, S., Shigetaro, Y., Mineichi, I., and Fujimoto, T., 1985, "Research on Idling Rattle of Manual Transmission," SAE Paper 850979.

Okada, Y., Nakamura, Y., and Tanaka, N., 1981, "Torsional Vibrational Absorber for Gear Transmission Systems," *Proceedings of the International Symposium of Gearing & Power Transmissions*, Tokyo, Japan.

Reik, W., 1986, "Torsional Vibration and Transmission Noise," LUK Technical Report.

Sakai, T., Doi, Y., Yamamoto, K., Ogasawara, T., and Narita, M., 1981, "Theoretical and Experimental Analysis of Rattling Noise of Automotive Gearbox," SAE Paper 810773.

Seaman, R. P., Johnson, C. E., and Hamilton, R. F., 1984, "Component Inertial Effects on Transmission Design," SAE Paper 841686.

Thomson, W. T., 1981, *Theory of Vibration with Applications*, 2nd Edition, Prentice-Hall, Englewood Cliffs, NJ.

Setter, R. P., 1969, "Gear Train Noise Manual," Cincinnati Milling Machine Company.

Wang, C. C., 1977, "Rotational Vibration with Backlash: Part 1," ASME Paper No. 77-DET-105.

Wang, C. C., 1980, "Rotational Vibration with Backlash: Part 2," ASME Paper No. 80-C2/DET-61.

Xie, H., 1987, "Analysis of Automotive Transmission Neutral Gear Rattle Problem," Masters Thesis, The Ohio State University.

Yang, D. C. H., and Lin, J. Y., 1987, "Hertzian Damping, Tooth Friction and Bending Elasticity in Gear Impact Dynamics," ASME JOURNAL OF MECHANISMS, TRANSMISSIONS, AND AUTOMATION IN DESIGN, Vol. 109, pp. 189-196.

APPENDIX

Equations for the No Impact Case

Type 1: $-\bar{b}_j \le \delta_{mj} \le \bar{b}_j$

Equations for the relative motion between the flywheel and clutch:

$$\delta_{m1} = \frac{\bar{F}_{m1}}{\alpha_1};\ \delta_{p1} = \frac{\bar{F}_{p1}}{\sqrt{(\alpha_1 - \bar{\Omega}_p^2)^2 + \eta^2}}$$

Equations for the relative motion between the gears:

$$\delta_{m3} = \frac{\bar{F}_{m3}}{\alpha_3};\ \delta_{p3} = \frac{\bar{F}_{p3}\left(\frac{N_{fp1}}{\alpha_3}\right)}{\sqrt{(N_{fp1} - \bar{\Omega}_p^2)^2 + \eta^2}}$$

Type 2: $\delta_{mj} \le -\bar{b}_j$ or $\delta_{mj} \ge \bar{b}_j$

Equations for the relative motion between the flywheel and clutch:

$$\delta_{m1} = \bar{F}_{m1} + (1-\alpha_1)\bar{b}_1;\ \delta_{p1} = \frac{\bar{F}_{p1}}{\sqrt{(1-\bar{\Omega}_p^2)^2 + \eta^2}}$$

Equations for the relative motion between the gears:

$$\delta_{m3} = \bar{F}_{m3} + (1-\alpha_3)\bar{b}_3;\quad \delta_{p3} = \frac{\bar{F}_{p3}(N_{fp1})}{\sqrt{(N_{fp1} - \bar{\Omega}_p^2)^2 + \eta^2}}$$

Equations for Two-Sided Impact Case

Equations for the relative motion between the flywheel and clutch:

$$\delta_{m1} = \frac{\bar{F}_{m1}}{1 - \frac{\bar{F}_{tsm1}}{\delta_{p1}}};\ \delta_{p1} = \frac{\bar{F}_{ts1}(1-\bar{\Omega}_p^2) \pm \sqrt{\bar{F}_{p1}^2(1-\bar{\Omega}_p^2) + [\bar{F}_{p1}^2 - \bar{F}_{ts1}^2]\eta^2}}{(1-\bar{\Omega}_p^2)^2 + \eta^2}$$

Equations for the relative motion between the gears:

$$\delta_{m3} = \frac{\bar{F}_{m3}}{1 - \frac{\bar{F}_{tsm3}}{\delta_{p3}}};\ \delta_{p3} = \frac{\bar{F}_{p3}(N_{fp1})}{\sqrt{(N_{fp1} - \bar{\Omega}_p^2)^2 + \eta^2}} + \bar{F}_{ts3}$$

$$\bar{F}_{tsmj} = \frac{2(\pi-2)}{\pi}(1-\alpha_j)\bar{b}_j;$$

$$\bar{F}_{tsj} = \frac{4}{\pi}(1-\alpha_j)\bar{b}_j\left[1 - \left(\frac{4-\pi}{4}\right)\left(\frac{\bar{b}_j^2 + 3\delta_{mj}^2}{\delta_{pj}^2}\right)\right]$$

Equations for Single-Sided Impact Case

Equations for the relative motion between the flywheel and clutch:

$$\delta_{m1} = \frac{\bar{F}_{m1} + \frac{(1-\alpha_1)}{2}\left(\bar{b}_1 - \frac{2\delta_{p1}}{\pi} - \left(\frac{\pi-2}{\pi\delta_{p1}}\right)(\bar{b}_1 - \delta_{m1})^2\right]}{\alpha_{A1}}$$

$$\delta_{p1} = \frac{\bar{F}_{ss1}(\alpha_A - \bar{\Omega}_p^2) \pm \sqrt{\bar{F}_{p1}^2(\alpha_{A1} - \bar{\Omega}_p^2) + [\bar{F}_p^2 - \bar{F}_{ss1}^2]\eta^2}}{(\alpha_{A1} - \bar{\Omega}_p^2)^2 + \eta^2}$$

Equations for the relative motion between the gears:

$$\delta_{m3} = \frac{\bar{F}_{m3} + \frac{(1-\alpha_3)}{2}\left[\bar{b}_3 - \frac{2\bar{\delta}_{p3}}{\pi} - \left(\frac{\pi-2}{\pi\bar{\delta}_{p3}}\right)(\bar{b}_3 - \delta_{m3})^2\right]}{\alpha_{A3}}$$

$$\delta_{p3} = \frac{1}{\alpha_{A3}}\left[\frac{\bar{F}_{p3}(N_{fp1})}{\sqrt{(N_{fp1} - \bar{\Omega}_p^2)^2 + \eta^2}} + \bar{F}_{ss3}\right]$$

$$\bar{F}_{ssj} = \frac{2}{\pi}(1-\delta_{mj})(1-\alpha_j)\left[1 - \left(\frac{4-\pi}{\pi}\right)\left(\frac{\bar{b}_j - \delta_{mj}}{\delta_{pj}}\right)^2\right]$$

$$\alpha_{Ai} = (1+\alpha_i)/2$$